Electronic structure and equilibrium properties of $Ga_xAl_{1-x}N$ alloys

E. A. Albanesi, W. R. L. Lambrecht, and B. Segall
Department of Physics, Case Western Reserve University, Cleveland, Ohio 44106-7079
(Received 22 July 1993)

First-principles calculations by means of the linear-muffin-tin-orbital method were carried out of the electronic band structures, equilibrium lattice constants, energies of formation, and bulk moduli of $Ga_xAl_{1-x}N$ alloys in zinc-blende-derived structures with a specific cation ordering. The miscibility and band-gap bowing of disordered alloys were studied using a cluster expansion method. Complete mutual solubility is predicted to occur at typical growth temperatures. The band gap is found to exhibit a weak bowing and to change from being indirect ($\Gamma \rightarrow X$) for $x = 0$ to direct at Γ at a concentration of $x \approx 0.4$.

I. INTRODUCTION

With the (room temperature) band gap varying from 3.4 eV in GaN to 6.2 eV in AlN, the $Ga_xAl_{1-x}N$ alloy system has great promise as a wide-band-gap semiconductor for optoelectronics.[1,2] This is particularly true because in their natural crystal structure (wurtzite) both AlN and GaN have direct band gaps. Recently, important progress has been made in epitaxial growth of semiconductor grade films of these materials [intrinsic carrier concentrations in the range 10^{16}–10^{17} cm^{-3} and mobilities up to 600 cm^2/Vs (Ref. 6)] and controlled p- (with Mg) (Refs. 3–5) and n-type (with Si) doping.[6] Light emitting diodes emitting in the UV/violet region have been fabricated from $Ga_xAl_{1-x}N$/GaN heterostructures and stimulated emission has been demonstrated by Akasaki and Amano.[6]

While both materials occur naturally in the hexagonal wurtzite structure, it has proven possible to stabilize the zinc-blende structure of GaN on GaAs {001} substrates[7–9] and on cubic SiC {001} substrates.[10] In fact, the existence of one-dimensional disorder in the cubic vs hexagonal stacking in GaN has been reported by Lei and Moustakas.[11] The only report of the existence of zinc-blende AlN that we are aware of is that of AlN precipitates formed by N-ion implantation in fcc Al.[12] Nevertheless, both for AlN and GaN the energy difference between the zinc-blende and wurtzite structures is very small [of the order of 10–15 meV/atom for GaN (Refs. 13 and 14) and 18 meV/atom for AlN (Ref. 14)]. It would thus appear possible to stabilize both in the zinc-blende structure. The existence of two different crystal structures with different electronic band structures, phonon scattering, etc., adds further versatility to this alloy system. Because of the higher symmetry, the zinc-blende form may have certain advantages such as higher drift velocity. Band structure calculations by Lambrecht and Segall,[15] however, predict that the band gap of cubic AlN would be indirect $\Gamma \rightarrow X$ and ~1 eV lower than for the wurtzite polytype. Cubic GaN, on the other hand, is predicted to be direct. The question thus arises for the $Ga_xAl_{1-x}N$ alloy system as to where the transition from the indirect to the direct band gap takes place.

In this paper, we present calculations of zinc-blende alloys of $Ga_xAl_{1-x}N$. Our first-principles calculations address both the miscibility and electronic properties. The approach is based on the cluster expansion method with the expansion parameters determined from calculations for the ordered structures at $x = 0, 0.25, 0.50, 0.75, 1$. We determine the concentration dependence of the conduction band minima at Γ and X relative to the valence band maximum, i.e., the relevant band gaps. Since the conduction band minimum at Γ changes very little between the wurtzite and zinc-blende structures, our results also provide an approximation for the direct band-gap behavior in wurtzite $Ga_xAl_{1-x}N$ alloys.

The computational approach is described briefly in Sec. II. Results for the equilibrium total energy properties of the ordered compounds are given in Sec. III A. The miscibility is disussed in Sec. III B. Results for the band structures, and, in particular, the band-gap behavior are presented in Sec. III C. The conclusions are summarized in Sec. IV.

II. COMPUTATIONAL METHOD

The approach utilized here to study the statistical mechanical properties of disordered alloys is the cluster expansion method of Sanchez and de Fontaine[16] and Sanchez *et al.*[17] As suggested by Connolly and Williams,[18] first-principles calculations of a set of ordered compounds are used to derive the coefficients of the cluster expansion. The cluster expansion was initially applied to binary alloys. The semiconductor alloys that we consider in this paper are strictly ternary alloys. However, because the energy costs of antisite defects are considerably higher than the relevant energies involved in the problem, i.e., the formation energies, we assume that the disorder occurs only on the cation sublattice. This reduces the problem to that of binary alloys on the face centered cubic (fcc) lattice, i.e., to a pseudobinary alloy. The properties of interest here are the energy of formation $\Delta E_f(x)$ and the band gap $E_G(x)$ at various k points as a function of concentration x in $Ga_xAl_{1-x}N$.

By truncating the cluster expansion at the level of

0163-1829/93/48(24)/17841(7)/$06.00 ©1993 The American Physical Society

nearest neighbor tetrahedron interactions, the problem can be reformulated as follows. For each of the five basic types of (cation) nearest neighbor tetrahedrons A_nB_{4-n}, with $n = 0,1,2,3,4$, there is a certain probability $P_n(x)$ of occurrence in the disordered alloy of concentration x. The property Ω is then expanded as follows:

$$\Omega(x) = \sum_n P_n(x)\Omega_n. \quad (1)$$

On the other hand, we can associate each tetrahedron with a well defined ordered compound: A_4 and B_4 with the pure fcc sublattice (here actually zinc blende when the counter anion is taken into account), A_2B_2 with the $L1_0$ ordering of the cation sublattice, and A_3B and AB_3 with the $L1_2$ ordering. Figures of these structures can be found for example in Ref. 19. In each of these, only the corresponding tetrahedron occurs. We can thus straightforwardly associate the property of the ordered compound with the property Ω_n of the corresponding tetrahedron. The procedure employed here is a special case of the more general approach in which the cluster expansion applied to a given set of ordered compounds is inverted to derive the interaction parameters. In a full-fledged application of the cluster variation method, one determines the probability of each cluster $P_n(x,T)$ by minimizing the free energy (at a given temperature T) with respect to the $P_n(x,T)$. Instead, for simplicity, we assume here a random (i.e., binomial) distribution function,

$$P_n(x) = \binom{4}{n} x^n(1-x)^{4-n}, \quad (2)$$

corresponding to the high temperature limit. We do not claim here that the above approach would be well converged at the tetrahedron level. In fact, the work of Wei *et al.*[19] indicates that longer range pair interactions can make significant contributions. Nevertheless, the above formulation provides us with a useful first approximation. We may also note that for those alloys that are not in thermodynamic equilibrium at the growth temperature, the distribution of clusters will deviate from that derived by the cluster variation method. A random distribution may in fact be more representative of the frozen-in disorder of the gas phase or liquid phase from which the solid solutions are quenched.

For the study of the properties of the ordered compounds, we employ the linear-muffin-tin-orbital method in the atomic sphere approximation (ASA) (Ref. 20) and the density functional theory in the local density approximation (LDA) (Ref. 21) using the Hedin-Lundqvist parametrization of exchange and correlation.[22] Since the zinc-blende structure is not close-packed, empty spheres were introduced in the interstitial region[23] and the combined correction was applied.[20] Monkhorst-Pack[24] sets of eight and six special k points were used, respectively, for the $L1_0$ and $L1_2$ structures leading to a convergence of better than 1 meV/atom.

The energies of formation are

$$\Delta E_f(x) = E_{\rm tot}({\rm Ga}_x{\rm Al}_{1-x}{\rm N}) - xE_{\rm tot}({\rm GaN}) - (1-x)E_{\rm tot}({\rm AlN}), \quad (3)$$

with the total energy $E_{\rm tot}$ normalized per atom. In order to ensure comparable **k**-sum convergence in all terms in (3), the calculations of $E_{\rm tot}$ for GaN and AlN were carried out in the same unit cell and with the same density of **k** points as the corresponding alloy.

III. RESULTS

A. Equilibrium properties of the ordered compounds

The total energy was calculated as a function of volume for each of the ordered compounds discussed above. The resulting equation of state was fitted to the equation of Rose *et al.*[25] in order to obtain the equilibrium lattice constant a_0, cohesive energy E_c, bulk modulus B_0, and its pressure derivative B'. The atomic total energies used in the calculation of the cohesive energy include a spin-polarization correction. These results are shown in Table I.

The lattice constant, bulk modulus, and its pressure derivative are all seen to follow a linear concentration dependence very closely. For the lattice constant, this corresponds to Vegard's law. The agreement with the available experimental data at the endpoints of the concentration range is satisfactory aside from the usual overestimate of the cohesive energy by the LDA.

B. Miscibility

The energies of formation are shown in Fig. 1. The positive values indicate a phase separation behavior of the alloy system. To within the estimated accuracy of our calculation, the energies of formation follow a parabola,

$$\Delta E_f(x) = 4\Delta E_2 x(1-x). \quad (4)$$

This indicates that the energetics of this system can approximately be mapped onto that of the ferromagnetic Ising model.[26] An estimate of the maximum of the miscibility gap (MG) is then given by

$$T_{\rm MG} \approx 0.8163 \times 2\Delta E_2/k, \quad (5)$$

TABLE I. Equilibirum properties of ordered $Ga_xAl_{1-x}N$ alloys. Experimental values are given in parentheses. For the lattice constant, it is the "cubic" value yielding a volume per atom equal to the measured volume for the wurtzite structure.

	a_0 (Å)	E_c (eV/atom)	B_0 (GPa)	B'
AlN	4.35 (4.37)[a]	6.40 (5.75)[b]	209 (210)[c]	3.9
$GaAl_3N_4$	4.39	6.04	208	4.0
$GaAlN_2$	4.43	5.69	206	4.2
Ga_3AlN_4	4.46	5.35	203	4.3
GaN	4.48 (4.50)[a]	5.02 (4.45)[b]	199 (190)[d]	4.4

[a]Reference 35.
[b]From enthalpies of formation given in Ref. 36.
[c]Reference 37.
[d]Reference 38.

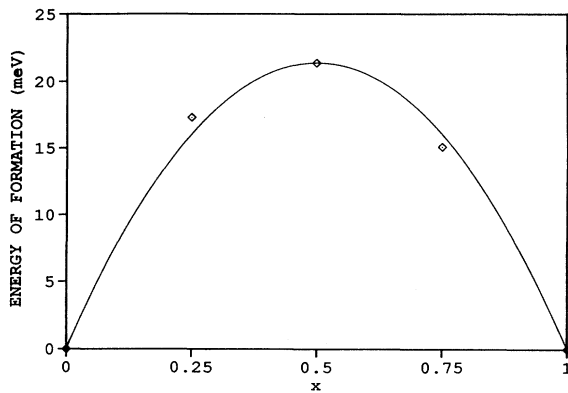

FIG. 1. Energy of formation of $Ga_xAl_{1-x}N$ alloys.

with k the Boltzmann constant. This is based on the regular solution model with a renormalization coefficient 0.8163, as explained in Ref. 26.

For the present systems this implies that $T_{MG} \approx 400$ K. This indicates very good solubility at moderately high temperatures. At typical growth temperatures, $T \geq 600\,^\circ$C, we can thus assume complete solubility. This implies that the high temperature random distribution function of the clusters that we will assume below for the band-gap behavior should be a fairly good approximation.

We note that our value of T_{MG} is probably an underestimate because the present calculation neglects the residual internal strains in the alloy. That is, we have implicitly assumed that each cluster takes the equilibrium volume per atom of the corresponding ordered compound. Because of the 3% lattice mismatch between AlN and GaN, the local clusters will occupy a volume intermediate between that of the ideal volume of each cluster and the volume corresponding to the average lattice constant of the alloy in which it occurs. As shown in a previous study of Ni_xPt_{1-x} alloys,[28] which involved much larger ($\approx 14\%$) lattice mismatches, this effect may lead to appreciable changes of the energies. Indeed, the elastic energy involved in compressing GaN and expanding AlN to the average lattice constants can easily be estimated from the bulk modulus. It is found to be of the same order of magnitude as the calculated energy of formation. This, however, is an overestimate since the energy will be lowered by the relaxations of the nearest neighbor Al-N and Ga-N bonds. But even with a change by a factor of 2 in the miscibility gap, our conclusion that there is good solubility at the growth temperatures remains valid. Finally, we note that typical growth methods used for these compounds may involve conditions removed from equilibrium. This makes an accurate determination of the miscibility gap temperature a less urgent issue. Further work will be necessary to obtain a more accurate value of the miscibility gap temperature.

C. Electronic band structure

The band structures of the ordered compounds are shown in Figs. 2–4. Strictly speaking all of these have

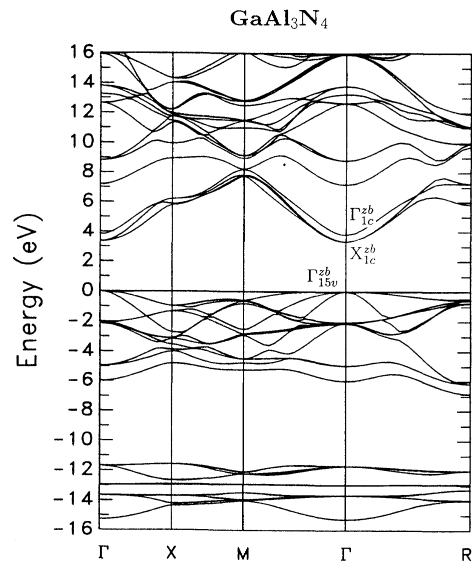

FIG. 2. Band structure of $GaAl_3N_4$ in the $L1_2$ cation ordered zinc-blende structure. The labels of the k points of the simple cubic Brillouin zone along the axes follow Ref. 29. The zinc-blende labels of specific eigenvalues are explained in the text.

direct band gaps at Γ. However, as we now discuss, some of these gaps are only "pseudodirect." By that we mean that the state at the conduction band minimum is related to a zinc-blende Brillouin zone (BZ) edge state (at X) folded onto the Γ point by the doubling or quadrupling of the cell. This implies that the corresponding wave functions show a strong similarity to the X^{zb}_{1c} state

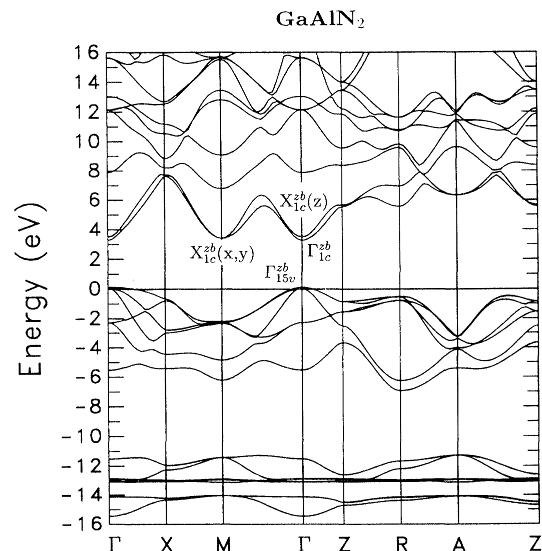

FIG. 3. Band structure of $GaAlN_2$ in the $L1_0$ cation ordered zinc-blende structure. The labels of the k points of the tetragonal Brillouin zone along the axes follow Ref. 29. The zinc-blende labels of specific eigenvalues are explained in the text.

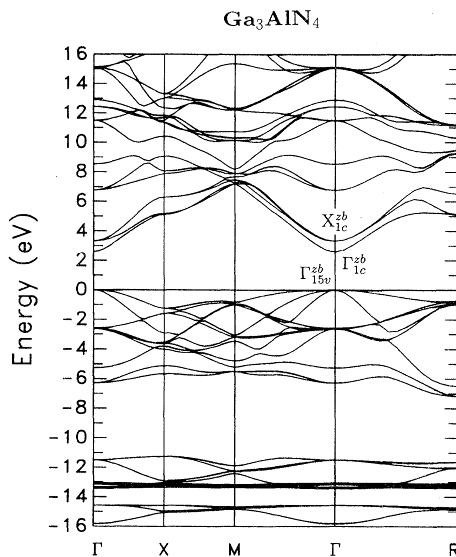

FIG. 4. Band structure of Ga_3AlN_4 in the $L1_2$ cation ordered zinc-blende structure. For labeling see Fig. 2.

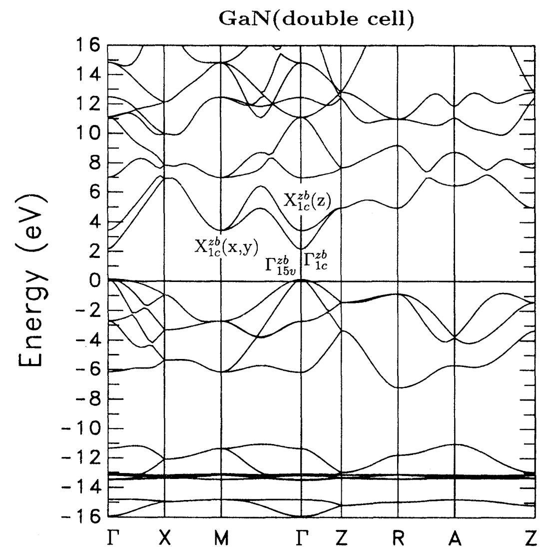

FIG. 5. Band structure of zinc-blende GaN in the tetragonal (doubled) unit cell and Brillouin zone. For labeling see Fig. 3.

of zinc blende and thus that the optical dipole matrix element can be expected to be smaller than those for an allowed gap in zinc blende. (To avoid confusion, we will indicate that the symmetry labeling and k-point notation corresponds to that for zinc blende by a superscript zb. Unsuperscripted k points correspond to the tetragonal or simple cubic BZ relevant for the 50% and for the 25% and 75% alloys, respectively.) The k-point notation of the simple cubic and tetragonal Brillouin zones follow Bradley and Cracknell.[29] The magnitude of the matrix element will depend on the difference of the Al and Ga potentials and on the extent of the relaxations from the ideal zinc-blende lattice positions.

To facilitate the comparison of the band structures of the alloys to those of the parent compounds AlN and GaN, it is useful to display the bands of the latter using the same Brillouin zone and unit cell as for the alloy. For example, the bands of GaN in the double cell are shown in Fig. 5. As is clearly evident, there is a great similarity to the bands of $GaAlN_2$ (Fig. 3) aside from the lifting of some degeneracies in $GaAlN_2$ due to a lowering of the symmetry. The lowest two conduction band states at Γ and M (of the tetragonal BZ) have been labeled using the notation of the zinc-blende (or fcc) BZ. The X_{1c}^{zb} state is seen to occur both at M and Γ of the tetragonal BZ. The state folded to Γ is the X_{1c}^{zb} state in the z direction. The doubly degenerate M conduction band minimum corresponds to the equivalent states of the x and y directions of the zinc-blende BZ. This is because the tetragonal unit cell is rotated 45° from the cubic axes (see Fig. 6). One can then see that the bands along $\Gamma - Z$ (tetragonal) are essentially the folded version of the $\Gamma^{\mathrm{zb}} - X^{\mathrm{zb}}$ bands. Along the tetragonal $\Gamma - M$ line one finds two sets of bands: the $\Gamma^{\mathrm{zb}} - X^{\mathrm{zb}}$ bands and the bands joining one X^{zb} state to another.

We note that in GaN the lowest conduction band is the $\Gamma_{1c}^{\mathrm{zb}}$ state, the next higher one being the X_{1c}^{zb} state. In AlN, the order is inverted. The reason for this has been discussed in Ref. 15. Basically the reason why the $\Gamma_{1c}^{\mathrm{zb}}$ state is deeper (relative to the X_{1c}^{zb} state) in GaN than in AlN is that the purely s-like $\Gamma_{1c}^{\mathrm{zb}}$ state is sensitive to the potential near the cation nucleus. Thus it is deeper for the element Ga which has the higher Z (Z being the atomic number). In a tight-binding description, the X_{1c}^{zb} state is an antibonding combination of anion s and cation p. In our LMTO-ASA expansion, it also has a significant weight in the interstitial (empty sphere) region. Because p-state wave functions vanish at the nucleus, they are less sensitive to the atomic number. Thus, the X_{1c}^{zb} states in GaN and AlN are more similar to each other than are the $\Gamma_{1c}^{\mathrm{zb}}$ states.

Returning to $GaAlN_2$, we find that the lowest conduction band state is symmetric with respect to the fourfold rotation inversion symmetry operation whereas the second one is odd. Indeed, the lower state has cation s contributions and no p_z, while the opposite is true for

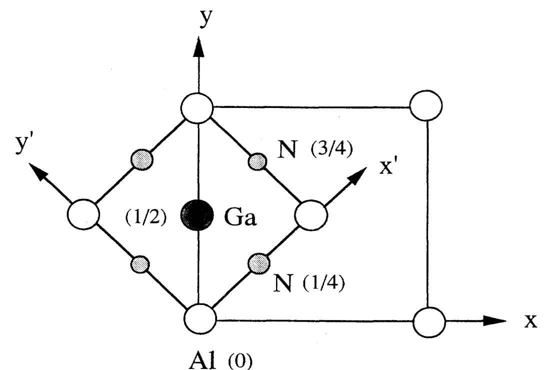

FIG. 6. Structure of the $L1_0$ structure in (001) projection.

the second one. Only the symmetric state is compatible with the Γ_{1c}^{zb} symmetry. Thus, we can identify the lower one as an "Γ_{1c}^{zb}-like" state and the second one as an "X_{1c}^{zb}-like" state. The X_{1c}^{zb}-like state is not exactly the same as the corresponding states at M because the symmetry between $\{x,y\}$ and z has been broken.

Similarly, we can identify the states in the Ga_3AlN_4 and $GaAl_3N_4$ band structures by comparison to those of GaN and AlN in the quadrupled (simple cubic) unit cell. The identification of the low-lying conduction band state at Γ is even more straightforward since the triply degenerate eigenvalue must clearly correspond to the three (x, y, and z) folded X_{1c}^{zb} states. We thus conclude that $GaAl_3N_4$ has only a pseudodirect, while the other two alloys have a direct band gap. This already indicates that the "indirect-to-direct" crossing takes place between $x = 0.25$ and $x = 0.50$.

Some amplification of the above statement is in order. As noted above, the matrix element at the pseudodirect transition in $GaAl_3N_4$ is not zero, and, depending on the strength of the perturbations, may not be very small. Furthermore, for the random alloys (i.e., for $x \neq 0.25$), the k-selection rule breaks down. Thus the transition between the "indirect" and "direct" gaps will not be sharp.

To determine the crossover more accurately, we use the cluster expansion method to extend our results to a continuous range of concentration values. Applying Eqs. (1) and (2) to the direct $\Gamma_{15v}^{zb} \rightarrow \Gamma_{1c}^{zb}$ and "indirect" $\Gamma_{15v}^{zb} \rightarrow X_{1c}^{zb}$ gaps , we obtain the results of Fig. 7. We see that both vary nearly linearly, i.e., there is negligible band-gap bowing. The X_{1c}^{zb} state remains almost constant with respect to the valence-band maximum while the Γ_{1c}^{zb} state decreases linearly from 4.26 eV in AlN to 1.97 eV in GaN. (These values correspond to the calculated equilibrium structures.) This is consistent with the anion-s–cation-p nature of the X_{1c}^{zb} state and the great similarity between Al and Ga p states mentioned earlier. A larger variation occurs in the s states for the reasons discussed above. The crossover from indirect to direct

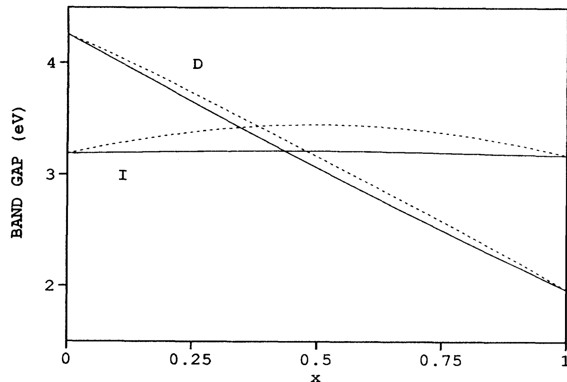

FIG. 7. Band-gap variation with concentration x in $Ga_xAl_{1-x}N$ alloys. The direct gap $\Gamma_{15v}^{zb} \rightarrow \Gamma_{1c}^{zb}$ is indicated by D and the "indirect" gap $\Gamma_{15v}^{zb} \rightarrow X_{1c}^{zb}$ by I. The full lines are the results for the ideal structures and the dashed lines are upper limit estimates for the distorted structure including bond length relaxation.

gap is found to occur at $x = 0.43$, corresponding to a maximum direct gap of 3.22 eV.

We note that all the band gaps reported here are underestimates because of the LDA. The band gap correction expected for AlN is 1.3 eV (i.e., the difference between the experimental and LDA value of the band gap for the wurtzite structure[15]) and 0.8 eV for GaN. The correction is expected to vary approximately proportionally to the band gap itself because it varies proportionally to the inverse of the dielectric constant.[30] Since the band gaps vary nearly linearly with concentration in the alloy system, the correction can also be expected to be linear in the concentration.

The band-gap bowing (i.e., deviation from linearity) found here is surprisingly small when compared to recent results for other wide-band-gap semiconductor alloy systems such as diamond/c-BN and SiC/BP.[26,27] In those cases, the band-gap bowing was associated with type-II band offsets at the corresponding heterojunctions. The band-offset at GaN/AlN heterojunctions has not yet been determined.

Another possible origin of band-gap bowing is bond-length relaxations. One may expect the Al-N and Ga-N bond lengths to relax towards their ideal values leading to a distortion of the structure. To make an estimate of this, consider a simple ball and spring model with central force constants. Assuming that only the N atom is displaced from its ideal position towards the Al and away from the Ga, one can easily show that minimization of the elastic energy would lead simultaneously to an ideal Ga-N and Al-N bond length. Inclusion of bond-bending forces and/or Ga-Ga and Al-Al forces will lead to deviations from this simple result. A compromise between the average bond length scaled by Vegard's law for the alloy's lattice constant and the equilibrium ideal lengths for each bond separately will be reached. To obtain an upper limit for the effects of the relaxation on the band-gap bowing, we have repeated the band structure calculations assuming relaxation to perfect Al-N bond lengths of 1.88 Å, and Ga-N bond lengths of 1.94 Å. As may be seen in Fig. 7, the resulting changes lead to a small upward bowing of the band gaps. The band-gap bowing parameters b_Γ and b_X defined by

$$E_G(x) = \overline{E}_G + \Delta E_G(x - 1/2) - bx(1 - x), \qquad (6)$$

with $\overline{E}_G = [E_G(1) + E_G(0)]/2$ and $\Delta E_G = E_G(1) - E_G(0)$, are $b_\Gamma = -0.40$ eV and $b_X = -0.92$ eV.

Finally, we note that the Γ_{1c}^{zb} conduction-band minimum and Γ_{15v}^{zb} valence-band maxima are very similar in nature to the corresponding states in the wurtzite structure. It is thus reasonable to consider their variation as an approximate model for the variation of the direct gap in wurtzite. The nearly linear variation of the direct band gap at Γ is qualitatively in agreement with the experimental data on wurtzite $Ga_xAl_{1-x}N$ (Refs. 31–33) which do not show any definitive indication of band-gap bowing to within the accuracy of the measurements. In Ref. 32 a weak upward bowing, i.e., a small negative b parameter, was obtained. It was also reported there that the lattice constant c did not vary linearly with composi-

tion. That is in contrast to most III–V alloys. This fact was believed to be a manifestation of the internal stress caused by the lattice mismatch between the $Ga_xAl_{1-x}N$ and the sapphire substrates. On the other hand, Khan *et al.*[34] obtained a weak downward bowing of the gap with a bowing parameter $b = 0.98$ eV. Those measurements, however, only covered the range $0.76 \leq x \leq 1$. Also, these authors reported that their x-ray analyses displayed a compositional fluctuation in their samples which increased with decreasing x.

The experimental results regarding band-gap bowing are thus inclusive except for the fact that the bowing is small. It could be dependent on the manner in which the samples are grown. Clearly more work in this area would be desirable. As we noted earlier, the actual values of the band gaps are not in agreement with experiment because of the LDA underestimate. As discussed above, however, this is not expected to change the band-gap bowing, nor the direct-indirect crossover.

IV. CONCLUSIONS

Linear-muffin-tin-orbital band structure and total energy calculations were performed for $Ga_xAl_{1-x}N$ alloys in zinc-blende-derived structures with $L1_2$ ordering of the cations at $x = 0.25$ and $x = 0.75$ and $L1_0$ ordering at $x = 0.5$. The lattice constant, bulk modulus and its pressure derivative, and the direct ($\Gamma \to \Gamma$) and indirect ($\Gamma \to X$) band gaps were found to vary nearly linearly with the concentration x. The energies of formation were found to be small and positive (of the order of 15–20 meV/atom) with an approximately parabolic concentration dependence. Using the cluster expansion method in the (cation) nearest neighbor tetrahedron approximation of Connolly and Williams,[18] these results were used to estimate the miscibility gap critical point of the disordered alloys. Although refinements of the calculation are necessary to obtain an accurate calculation of the latter, we can safely conclude that full miscibility can be assumed at the typical growth temperatures. The nature of the minimum band gaps of the ordered compounds, pseudodirect $\Gamma \to X$ or direct at Γ, was determined by comparison to the band structures of the parent compounds and inspection of the wave functions and their symmetries. Using a cluster expansion assuming a random occurrence of the cation nearest neighbor tetrahedral clusters, we deduce an indirect-to-direct crossover at $x \approx 0.43$. The band-gap bowing is found to be very small and positive even when atomic bond-length relaxation effects are included. The nearly linear behavior of the direct gap at Γ is in agreement with experimental data on the wurtzite alloys.

ACKNOWLEDGMENTS

This work was supported by NSF Grant No. DMR-92-22387. E.A.A. acknowledges financial support from the Consejo Nacional de Investigaciones Científicas y Técnicas, Argentina.

[1] *Wide Band Gap Semiconductors*, edited by T. D. Moustakas, J. I. Pankove, and Y. Hamkawa, MRS Symposia Proceedings No. 242 (Materials Research Society, Pittsburgh, 1992).

[2] *Wide-Band-Gap Semiconductors, Proceedings of the 7th Trieste Semiconductors Symposium*, edited by G. Van der Walle (North-Holland, Amsterdam, 1993) [Physica B **185**, 1–607 (1993)].

[3] H. Amano, M. Kito, and K. Hiramatsu, Jpn. J. Appl. Phys. **28**, L2112 (1989).

[4] S. Nakamura, M. Senoh, and T. Mukai, Jpn. J. Appl. Phys. **30**, L1708 (1991).

[5] R. J. Molnar and T. D. Moustakas, Bull. Am. Phys. Soc. **38**, 445 (1993).

[6] I. Akasaki and H. Amano, in Ref. 1, p. 383.

[7] M. Mizuta, S. Fujieda, Y. Matsumoto, and T. Kawamura, Jpn. J. Appl. Phys. **25**, L945 (1986).

[8] G. Martin, S. Strite, J. Thornton, and H. Morkoç, Appl. Phys. Lett. **58**, 21 (1991).

[9] S. Strite, J. Ruan, Z. Li, A. Salvador, H. Chen, D. J. Smith, W. J. Choyke, and H. Morkoç, J. Vac. Sci. Technol. B **9**, 1924 (1991).

[10] M. J. Paisley, Z. Sitar, J. B. Posthill, and R. F. Davis, J. Vac. Sci. Technol. A **7**, 701 (1989).

[11] T. Lei and T. D. Moustakas, in Ref. 1, p. 433.

[12] D. Schwabe and W. Mader, in *Proceedings of the First European Conference on Advanced Material Processes*, edited by H. E. Exner and V. Schumacher (DGM Informationsges., Oberursel, Germany, 1990), Vol. 2, pp. 1267–1272.

[13] A. Muñoz and K. Kunc, Phys. Rev. B **44**, 10 372 (1991); Physica B **185**, 422 (1993).

[14] C. -Y. Yeh, Z. W. Lu, S. Froyen, and A. Zunger, Phys. Rev. B **46**, 10 086 (1992).

[15] W. R. L. Lambrecht and B. Segall, in Ref. 1, p. 367.

[16] J. M. Sanchez and D. de Fontaine, in *Structure and Bonding in Crystals*, edited by M. O'Keeffe and A. Navrotsky (Academic Press, New York, 1981), Vol. 2, p. 117.

[17] J. M. Sanchez, F. Ducastelle, and D. Gratias, Physica **128A**, 334 (1984).

[18] J. W. D. Connolly and A. R. Williams, Phys. Rev. B **27**, 5169 (1983).

[19] S. -H. Wei, L. G. Ferreira, and A. Zunger, Phys. Rev. B **41**, 8240 (1990).

[20] O. K. Andersen, Phys. Rev. B **12**, 3060 (1975); O. K. Andersen, O. Jepsen, and M. Šob, in *Electronic Band Structure and its Applications*, edited by M. Yussouff (Springer, Heidelberg, 1987).

[21] P. Hohenberg and W. Kohn, Phys. Rev. **136**, B864 (1964); W. Kohn and L. J. Sham, *ibid.* **140**, A1133 (1965).

[22] L. Hedin and B. I. Lundqvist, J. Phys. C **4**, 2064 (1971).

[23] D. Gloetzel, B. Segall, and O. K. Andersen, Solid State Commun. **36**, 403 (1980).

[24] H. J. Monkhorst and J. D. Pack, Phys. Rev. B **13**, 5188 (1976).

[25] J. H. Rose, J. R. Smith, F. Guinea, and J. Ferrante, Phys. Rev. B **29**, 2963 (1984).

[26] W. R. L. Lambrecht and B. Segall, Phys. Rev. B **47**, 9289 (1993).

[27] E. A. Albanesi, W. R. L. Lambrecht, and B. Segall, Bull. Am. Phys. Soc. **38**, 566 (1993).
[28] C. Amador, W. R. L. Lambrecht, and B. Segall, Phys. Rev. B **47**, 15 276 (1993).
[29] C. J. Bradley and A. P. Cracknell, *The Mathematical Theory of Symmetry in Solids: Representation Theory for Point Groups and Space Groups* (Clarendon Press, Oxford, 1972).
[30] F. Bechstedt and R. Del Sole, Phys. Rev. B **38**, 7710 (1988).
[31] B. Goldenberg (private communication).
[32] S. Yoshida, S. Misawa, and S. Gonda, J. Appl. Phys. **53**, 6844 (1982).
[33] M. A. Khan, R. Skogman, R. Schulge, and M. Gerschenzon, Appl. Phys. Lett. **43**, 492 (1983).
[34] M. R. Khan, Y. Koide, H. Itoh, N. Sawaki, and I. Akasaki, Solid State Commun. **60**, 509 (1986).
[35] R. W. Wyckoff, *Crystal Structures*, 2nd ed. (Interscience Publishers, New York, 1964), Vol. 1.
[36] *CRC Handbook of Chemistry and Physics*, 68th ed., edited by R. C. Weast (CRC Press, Boca Raton, FL, 1988).
[37] W. Wettling and J. Windscheif, Solid State Commun. **50**, 33 (1984).
[38] D. Gerlich, S.L. del Sole, and G. A. Slack, J. Phys. Chem. Solids **47**, 437 (1986).